Fibers and Polymers 2010, Vol.11, No.7, 967-975 DOI 10.1007/s12221-010-0967-y

Nano Titanium Dioxide on Wool Keratin as UV Absorber Stabilized by Butane Tetra Carboxylic Acid (BTCA): A Statistical Prospect

Majid Montazer*, Esfandiar Pakdel[1], and Mohammad Bameni Moghadam[2]

Textile Department, Amirkabir University of Technology, Center of Excellence in Textile, Tehran, Iran
[1]Textile Department, Science and Research Branch, Islamic Azad University, Tehran, Iran
[2]Alame Tabatabaie University, Tehran, Iran

(Received December 8, 2009; Revised July 25, 2010; Accepted August 3, 2010)

Abstract: Photo yellowing of wool is one of the most important problems which have negative impacts on various aspects of wool prompting scientists to find a solution over the past decades. In this research the protective features of nano-titanium dioxide particles against UV on wool fabric were discussed and the color variations of wool samples after UV irradiation were measured and reported. It was shown that nano TiO_2 is a suitable UV absorber and its effect depends on the concentration. Also, it was assumed that butane tetracarboxylic acid plays a prominent role as a cross-linking agent to stabilize the nano-titanium dioxide as well as a polyanion to maintain negative charges on the wool surface for higher nano particles absorption. Also the variables conditions were optimized using response surface methodology (RSM).

Keywords: Nano TiO_2, Butane tetracarboxylic acid, Wool, UV absorber, Response surface methodology

Introduction

Titanium dioxide (TiO_2) is one of the most favorable semiconductors that have great photo-catalytic properties [1]. Due to its high photo-catalytic activity, non-toxicity, and physicochemical stability, its application has been increased [2,3]. As TiO_2 absorbs UV rays with wavelength higher than its band gap (E_g=3.2 eV), photo-catalytic properties can be observed; subsequently, transfer of electrons from valence band to conduction band occurs, resulting in the production of negative electrons and positive holes (e^-/h^+) are produced [4-6]. According to this mechanism, in the presence of oxygen and water molecules, hydroxyl radicals ($OH^·$) and superoxide radical anions ($O_2^·$) are produced [7]. Titanium dioxide exists in three different crystalline forms, i.e., anatase, rutile and brookite [7,8]. It has been proved that anatase form exhibits a higher level of photo-catalytic properties and it is more suitable for practical applications [8].

Generally, photo degradation products are colorful speices which are mainly yellow [9]. Wool is a natural fiber that undergoes photo oxidation when exposed to sunlight [9]. The tendency towards photo-yellowing of some textile fibers commonly used for apparel matches the following order: wool and silk >> nylon > cotton and other cellulosic fibers > polyester [10]. Wool fiber consists of three main parts: cortical cells, cuticle cells and cell membrane complex [11]. It has been confirmed that by hydrolyzing wool fibers different amino acids can be achieved [12]. A common and important feature of wool is that the protein chains are cross-linked by disulphide bonds [13]. Many chemical and physical changes occur on wool fibers via photo oxidation, one of which is photo-yellowing and others are loss of tensile strength and abrasion resistance and altered dyeing properties [9]. Some amino acids such as tryptophane, histidine and cystine undergo degradation processes [14].

Solar rays hitting the earth have wavelengths between 290 to 3000 nm and they are divided into three main parts: IR, visible rays, and UV [15]. The UV region can be further subdivided into four ranges, UV-A (320-400 nm), UV-B (280-320 nm), UV-C (200-280 nm), and Vacuum UV (10-200 nm) [16]. Majority of UV-C rays are absorbed by the stratosphere; therefore, UV rays hitting the earth have wavelengths between 290-400 nm [15].

Schefer earlier used as a white pigment reporting that titanium dioxide reduced the photo-yellowing of wool [16]. Qi produced self-cleaning cotton fabrics through applying nano particles of titanium dioxide of the surface of cotton [17]. Daoud produced self-cleaning keratinous fabrics by sol-gel method using TiO_2 [18]. In similar research which has been done by Montazer and Pakdel, reducing photo-yellowing on treated wool samples with three different concentrations of TiO_2 was evaluated [19]. The same group evaluated self-cleaning property of treated samples with TiO_2 and results were in consistent with previous findings. In those studies nano particles were stabilized on the fabric surface through citric acid instead of BTCA, in addition, they proved that oxidation process has increasingly impact on nano particles absorption [20].

Understanding the mechanism of photo-degradation and finding how to decrease photo-degradation are very important in protein fiber science. There are a few studies regarding the effect of titanium dioxide on photo-degradation of protein fabrics. Though there are several approaches by which the enhancement of the photo-stability of wool can be achieved, it is necessary to find new methods to prevent photo-yellowing. The aim of this work is to prevent photo-

*Corresponding author: tex5mm@aut.ac.ir

yellowing through increasing the photo-stability of wool using stabilized nano titanium dioxide as UV absorber.

With the purpose of linking titanium dioxide nano particles on wool surface more efficiently, cross-linking agent was used. 1,2,3,4-butane tetracarboxylic acid (BTCA) and sodium hypophosphite (SHP) were employed as a cross-linking agent and a catalyst, respectively. Ester cross-links have been researched for the benefit of not using formaldehyde [21-28]. This paper presents a study on the effect of TiO_2 concentration on reducing the photo-yellowing rate using the response surface methodology (RSM). The purpose of this study was to investigate the effects of both nano-titanium dioxide and cross-linking agent (BTCA) concentration on photo-stability of wool fabrics through evaluating data variations of whiteness and yellowness after UV irradiation. Their effects were analyzed using RSM due to its reasonable distribution of data points throughout the region of interest. RSM also allows model adequacy including lack of fit, designs of higher order to be built up sequentially, and provides an internal estimate of error. In addition, response surface designs do not require a large number of runs and too many levels of independent variables [29,30].

Optimization Methodology

In this work, it is assumed that the responses are modeled by estimating the coefficients of the second-order model as follows:

$$y = \beta_o + \sum_{i=1}^{k} \beta_i x_i + \sum_{i=1}^{k} \beta_{ii} x_i^2 + \sum_{i<j=2}^{k} \sum^{k} \beta_{ij} x_i x_j + \varepsilon \quad (1)$$

In equation (1), y is the measured response, x_i and x_j are the independent variables, β_i, β_{ii}, and β_{ij} are the model coefficients, ε is the error and k is the number of the independent variables (factors). The polynomial function (equation (1)) is an approximation of the true response function for a given response over the entire range of independent variables. If the range is restricted to a relatively small region, the approximation is usually in good agreement with the true response function and can be used in analysis, simulation, and optimization, etc. of the process [31]. The success of the RSM depends on the approximation of (y) by a low order polynomial in some region of the independent variables.

Finding optimal operating conditions for a given process using the response surface methodology yields a set of independent variables that minimize or maximize the responses predicted by the polynomial approximation. In general, the simultaneous optimization of multiple responses predicted by the second-order models is considered to be a nonlinear multi-objective optimization problem [31,32].

In this study, whiteness and yellowness variations were independent variables processed for equation (1) including ANOVA to obtain the interaction between the process variables and the responses. The quality of the fit of polynomial model was expressed by the coefficient of determination R^2 and R^2_{adj} in equations (2) and (3), respectively. The statistical significance was checked with an adequate precision ratio in equations (4) and (5), and by *DF* values and p values:

$$R^2 = 1 - \frac{SS_{residual}}{SS_{model} + SS_{residual}} \quad (2)$$

$$R^2_{adj} = 1 - \frac{SS_{residual}/DF_{residual}}{(SS_{model} + SS_{residual})/(DF_{model} + DF_{residual})} \quad (3)$$

$$Adequate\ precision = \frac{\max(\hat{Y}) - \min(\hat{Y})}{\sqrt{\overline{V}(\hat{Y})}} \quad (4)$$

$$\overline{V}(\hat{Y}) = \frac{1}{n}\sum_{1=1}^{n} V(\hat{Y}) = \frac{p\sigma^2}{n} \quad (5)$$

In equations (2) and (3), *SS* is the sum of squares, *DF* the degrees of freedom, p the number of model parameters, the residual mean square from ANOVA table, and n is the number of experiments.

Experimental

Materials

The 100 % raw wool fabric with twill structure and yarn fineness 30 (Nm) for warp and weft, fabric mass 350 g/m^2, warp and weft yarn density 16.2 and 15.1 per cm, respectively, was used. Nano powder of titanium dioxide (Degussa-p-25) was used as a UV absorber and its average particle size was around 21 nm. The nano-crystalline titanium dioxide used in wool doping has a large surface area and consists of a mixture of anatase and rutile phases. Butane tetracarboxylic acid ($C_6H_{10}O_8$) from Merck (Germany) was used as a cross-linking agent and sodium hypophosphite ($NaH_2PO_2 \cdot H_2O$) from Riedl-de-haen (Germany) was used as a catalyst. The ultrasonic bath was used to mix the components and a curing oven with a mechanical circulation of air was used.

Two UV-C (G8T4) bulbs from Philips (the Netherlands) were used as artificial UV sources. Ultrascan Hunter Lab XE was used as a spectrophotometer by using D65 source, 10 ^{o} collection angle and its detection territory was between 400 to 700 nm.

An IR spectroscopic analysis was performed using a Thermonikolet-Nexus 870 spectrophotometer (USA). SEM images and EDS patterns were achieved by Leo-440-I.

$KMnO_4$ Treatment

The scoured wool samples were treated with 3 % $KMnO_4$ in acidic solution (pH=4) in presence of 10 g/*l* NaCl. In order to adjust the pH, 4 N sulfuric acid was used. The treatment was conducted for 20 min in L.R.: 40:1. Cystin, tyrosine, and tryptophan were greatly affected by the

$KMnO_4$ treatment [33]. Nitrogen and sulfur contents decreased with increased extent of $KMnO_4$ treatment [33]. The brown color of oxidized wool was caused by MnO_2 ions. In order to remove the brown color from oxidized samples, they were treated with sodium bisulphite along with 0.5 m*l* of 4 N H_2SO_4 for 15 min. Finally the samples were washed thoroughly with warm (40 °C) and cold (22 °C) water and then dried at room temperature for 24 h. Additionally, all the treatments were carried out in an ultrasonic bath.

Nano TiO_2 Treatment

Nano TiO_2 particles were applied on the oxidized wool in various concentrations (Table 1). Impregnating bath was made of cross-linking agent (BTCA), sodium hypophosphite (SHP), and nano powder of titanium dioxide. The bath was sonicated for 10 min without wool sample and then the fabric was entered. The treated samples were cured at 120 °C for 2 min [34]. Then samples were irradiated with UV-C rays produced by Philips G8T5 for 3 h.

Results and Discussions

In this study, the central composite design (CCD) and response surface methodology (RSM) were applied to optimize the two most important operating variables: nano-titanium dioxide and cross-linking agent (BTCA). 20 experimental runs were conducted (Table 1). Independent variables were the amount of nano titanium dioxide powder (*A*), concentration of cross-linking agent (BTCA) in an impregnating bath (*B*), and ultrasonic time (*C*). The highest and lowest ranges of independent variables were presented in Table 2. For the treated oxidized wool samples, two response surfaces variations, Y_1 and Y_2 were discussed, where Y_1 is whiteness variation of treated oxidized wool after 3 h UV irradiation and Y_2 is yellowness variation of treated oxidized wool after 3 h UV irradiation. For all of the samples, the whiteness and yellowness measured by spectrophotometer (Ultrascan Hunter Lab XE) were shown according to YIE 313 and WIE 313 in Table 1.

Two equations were calculated (equations (6) and (7)) with their related response as a function of its independent variables. These equations could be used in predicting the response for the given values of TiO_2 and BTCA and ultrasonic bath time. According to these equations, response surfaces are shown in Figures 1 and 2.

Table 1. Experimental design with some results based on CCD

Run	*A*	*B*	*C*	Y_1	Y_2
1	0.38	10.5	32	33.39	11.93
2	0.6	16.00	16	35.04	11.6
3	0.38	10.50	32	33.46	11.89
4	0.6	5.00	48	35.56	11.56
5	0.38	10.5	5	33.77	12.01
6	0.16	5.00	16	27.58	14.29
7	0.6	5.00	16	34.34	12.18
8	0.75	10.50	32	36.75	11.42
9	0.01	10.50	32	19.72	17.08
10	0.38	10.50	59	34.05	12.58
11	0.38	10.50	32	32.54	12.74
12	0.6	16.00	48	36.92	11.49
13	0.38	1.25	32	30.58	13.46
14	0.16	5.00	48	29.8	13.67
15	0.16	16.00	48	32.24	12.78
16	0.38	10.50	32	33.23	11.98
17	0.16	16.00	16	31.6	13
18	0.38	19.75	32	36.04	11.8
19	0.38	10.50	32	32.74	12.78
20	0.38	10.50	32	33.12	12.49

Table 2. Minimum and maximum levels of Independent variables

Independent variable	Low level	High level
TiO_2 (g/*l*)	0.01	0.75
BTCA (%)	1.25	19.75
Ultrasonic time (min)	5	59

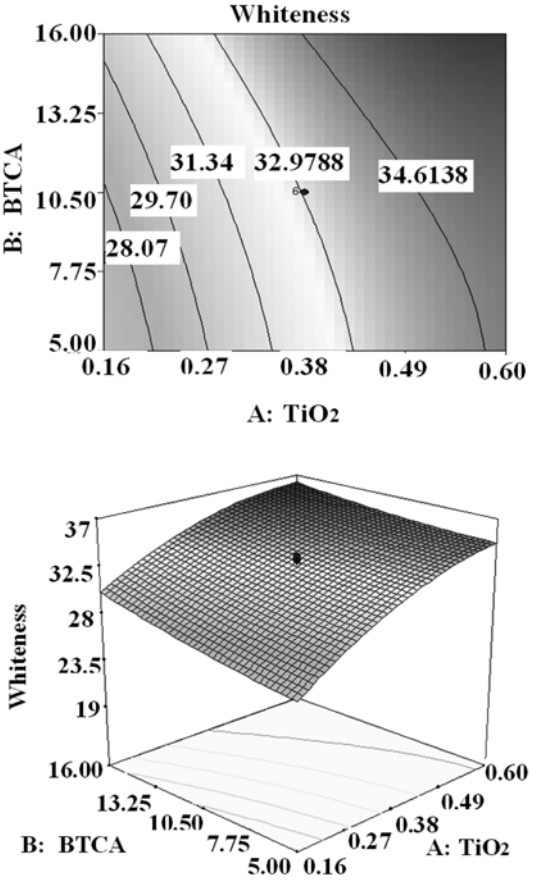

Figure 1. Response surface for whiteness as a function of TiO_2 and BTCA.

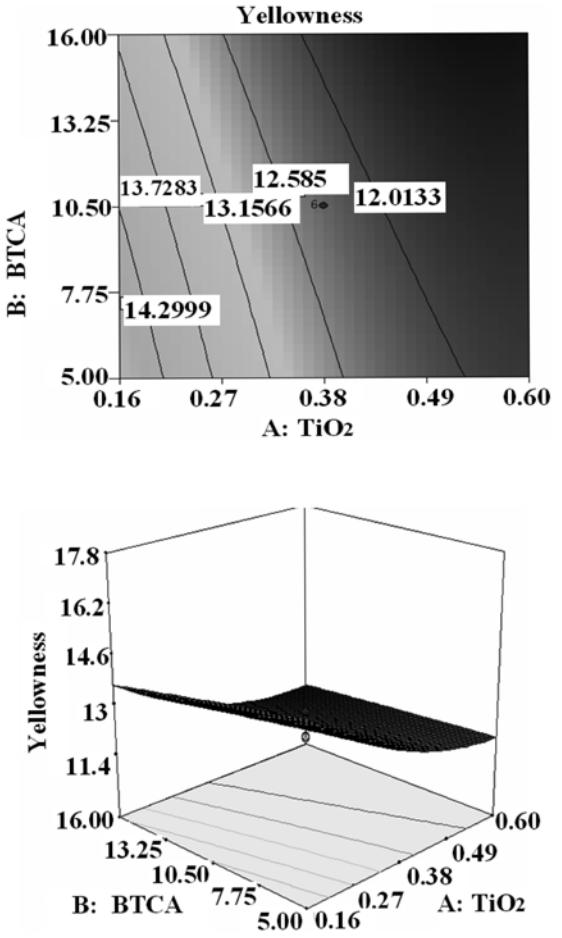

Figure 2. Response surface for yellowness as a function of TiO_2 and BTCA.

$$Y_1 = 33.04 + 3.61\,(A) + 1.3\,(B) + 0.47\,(C) - 0.55\,(AB) + 0.03\,(AC) - 0.11\,(BC) - 1.47\,(A2) + 0.32\,(B2) + 0.53\,(C2) \quad (6)$$

$$Y_2 = 12.32 - 1.29\,(A) - 0.41\,(B) - 0.045\,(C) + 0.19\,(AB) + 0.014\,(AC) + 0.11\,(BC) + 0.68\,(A2) - 0.024\,(B2) - 0.14\,(C2) \quad (7)$$

Response surface methodology (RSM) is a collection of mathematical and statistical techniques useful for designing experiments, building models, evaluating the effects of variables and searching optimum conditions of variables to predict targeted responses [35]. RSM has an important application in the process design and optimization as well as the improvement of existing design. This methodology is more practical compared to other approaches as it arises from experimental methodology which includes interactive effects among the variables and, eventually, it depicts the overall effects of the parameters on the process [36]. Analysis of variance (ANOVA) was used for analyses of the data to obtain interaction between the process variables and the responses.

The statistical significance and goodness of fit for the used models were evaluated by analyzing the variance (ANOVA) as presented in Tables 3 and 4. The lack of fit describes the variation of data around the fitted model [33]. If the model does not fit the data well, this will be significant [32,33]. It was observed that designed model for whiteness is statistically significant at F- value of 9.66 and values of prob>F (0.0007) (Table 3). As for yellowness, it was observed that the chosen model was significant at F-value of 5.78 and values of prob>F (0.0056) (Table 4). The fit of the model can be evaluated through *R*-squared coefficient, the results of Tables 3 and 4 indicated that only 10.32 and 16.13 % of

Table 3. ANOVA results for whiteness variations after 3 h UV irradiation

Source	Sum of squares	*DF*	Mean square	*F* value	*p*-value Prob>*F*	
Model	246.73	9	27.41	9.66	0.0007	Significant
A - TiO_2	177.83	1	177.83	62.64	>0.0001	
B - BTCA	22.95	1	22.95	8.08	0.0175	
C - Time	3.03	1	3.03	1.07	0.3260	
AB	2.42	1	2.42	0.85	0.3776	
AC	0.0072	1	0.0072	0.002	0.9608	
BC	0.11	1	0.11	0.037	0.8508	
A^2	31.21	1	31.21	11.00	0.0078	
B^2	1.50	1	1.50	0.53	0.4840	
C^2	4.12	1	4.12	1.45	0.2560	
Residual	28.39	10	2.84			
Lack of fit	27.72	5	5.54	41.26	0.0005	Significant
Pure error	0.67	5	0.13			
Cor total	275.12	19				

R-squared: 0.8968, Adjusted *R*-squared: 0.8040, CV%: 5.16.

Table 4. ANOVA results for yellowness variations after 3 h UV irradiation

Source	Sum of squares	*DF*	Mean square	F value	*p*-value Prob > *F*	
Model	32.83	9	3.65	5.78	0.0056	Significant
A - TiO_2	22.78	1	22.78	36.09	0.0001	
B - BTCA	2.31	1	2.31	3.67	0.0846	
C - Time	0.027	1	0.027	0.043	0.8393	
AB	0.29	1	0.29	0.46	0.5115	
AC	0.0015	1	0.0015	0.0023	0.9619	
BC	0.1	1	0.1	0.16	0.6941	
A^2	6.59	1	6.59	10.44	0.0090	
B^2	0.0081	1	0.008	0.013	0.9117	
C^2	0.29	1	0.29	0.46	0.5122	
Residual	6.31	10	0.63			
Lack of fit	5.44	5	1.09	6.20	0.0333	Significant
Pure error	0.88	5	0.18			
Cor total	39.14	19				

R-squared: 0.8387, Adjusted *R*-squared: 0.6935, CV%: 6.27.

total variables for whiteness and yellowness models, respectively, can not be explained by these models [33,35]. Through Adjusted *R*-squared it was confirmed that the model of whiteness has higher significance in comparison with the model of yellowness [33,35]. Low values of the coefficient of variation (CV %) for both models indicated a good precision and reliability of the experiments [33,35].

An equation was achieved for both whiteness and yellowness based on the virtual results. According to these equations relationships between independent variables and respond surfaces were known. Among the surface responses, yellowness must be minimized and whiteness is suitable to be maximized.

According to equations (6) and (7), the variation rate of whiteness and yellowness after UV irradiation were determined and the relation between the respond surfaces and independent variations were detected (Figures 1-4). These results show that whiteness and yellowness variations are not linear and it depends on the concentration of titanium dioxide absorbed on the wool as well as the concentration of cross-linking agent. Through increasing the concentration of nano titanium dioxide in the impregnating bath, higher absorption of TiO_2 on wool fabrics can be expected. As a result, wool surface was covered more in comparison with the low concentration; subsequently, the UV stability of treated samples improved and their color variations decreased significantly. On the other hand, it can clearly be seen that with low concentration of TiO_2 an adequate amount of titanium dioxide cannot be absorbed on the surface of wool samples; therefore, they cannot protect fabric against UV rays and as a result the photo-yellowing was higher and it has adverse effects on

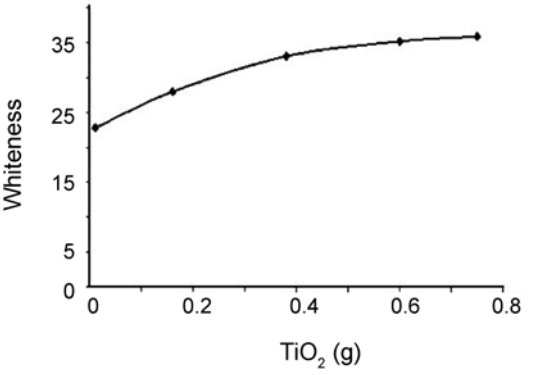

Figure 3. Whiteness as a function of TiO_2.

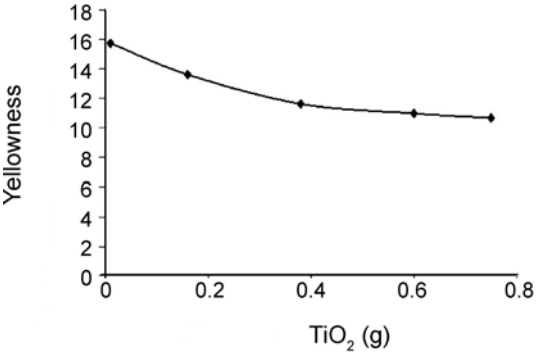

Figure 4. Yellowness as a function of TiO_2.

wool applications. Results of Figures 1 and 2 depicted that in those samples treated with high amount of TiO_2 and cross-linking agent (BTCA), after 3 h of UV irradiation by two

Table 5. Optimum conditions for independent variables and response surfaces

TiO_2 (g/*l*)	BTCA (%)	Time (min)	Whiteness	Yellowness	Desirability
0.6	12.94	16	35.65	11.44	0.74

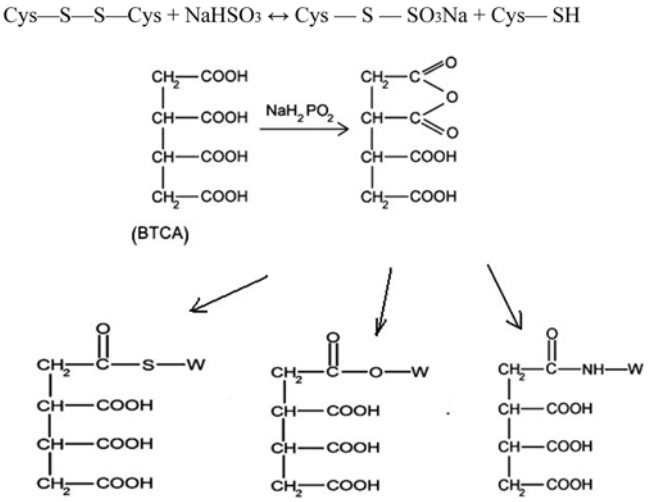

Scheme 1. Mechanism of reaction between wool and BTCA.

Philips bulbs 8W, the wool whiteness and yellowness was in maximum and minimum ranges respectively. Results of Table 5 illustrated that the optimum range of whiteness and yellowness can be achieved by 0.6 g/*l* TiO_2 and 12.94 % BTCA.

It has been proved that oxidation of wool with potassium permanganate can be an effective method to increase the rate of the absorption of cross-linking agents on the wool surface and consequently nano-particles with great tendency towards hydroxyl and carboxyl groups. In fact, oxidation can provide more suitable sites for creating covalent bonds between wool surfaces and cross-linking agents. By using the poly carboxylic cross-linking agent an extra carboxyl and hydroxyl groups were introduced on the wool surface leading to a higher absorption of nano TiO_2. The mechanism reaction between wool and of cross-linking agent (BTCA) illustrated in Scheme 1.

UV Reflectance Spectra

UV reflectance spectra of semiconductors can be explained by their solid band structure [37]. There are some useful UV blockers that were divided into organic and inorganic [37]. Titanium dioxide belongs to the inorganic UV blocking semiconductors [38]. UV absorption property is a natural attribute of TiO_2 which can be explained by the solid band theory. Figures 5 and 6 show the UV reflectance of wool samples in different conditions and various regions.

Results of Figures 5 and 6 demonstrated that raw wool can absorb some parts of UV-rays. Generally, TiO_2 particles are good UV absorber and they can protect fabrics from photo-oxidation. The lowest reflectance of treated samples is between 300 and 350 nm. Above 400 nm, the sample with a higher amount of TiO_2 had a lower range of reflectance. Results show that treated fabrics with TiO_2 are protected against photo-yellowing and the rate of yellowing decreases in contrast to untreated wool. This demonstrates the UV absorbance properties of TiO_2. Titanium dioxide acts primarily as a UV absorber resulting in a slower photo-yellowing rate. The results are consistent with the previous findings [38].

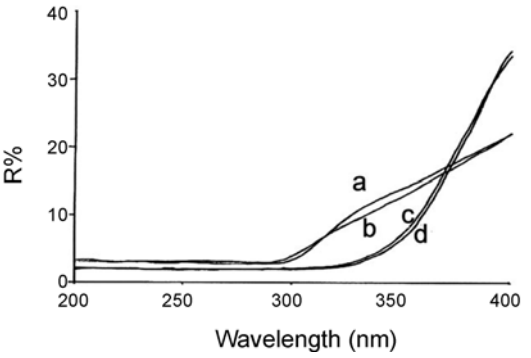

Figure 5. UV reflectance spectra of different wool samples (200-400 nm); (a) raw wool, (b) oxidized wool, (c) treated sample with 0.38 g/*l* TiO_2, and (d) treated sample with 0.75 g/*l* TiO_2.

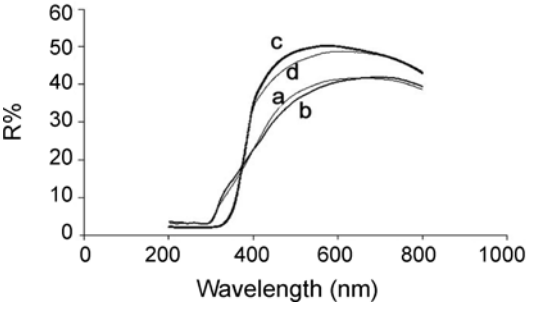

Figure 6. UV reflectance spectra of different wool samples (200-800 nm); (a) raw wool, (b) oxidized wool, (c) treated sample with 0.38 g/*l* TiO_2, and (d) treated sample with 0.75 g/*l* TiO_2.

FTIR and Raman Spectra

Infrared spectroscopy is a common technique for studying chemical structure of wool. Raman spectroscopy seems to be a useful method of observing the conformational changes in proteins [39]. Through Raman and FT-IR spectra of wool samples, the influence of applied nano particles and cross-linking agent on the chemical structure and oxidation process of wool fibers during UV irradiation was investigated. The analysis of band intensity of Raman spectra for disulphide bonds in untreated samples shows an appearance of band in the region of 480-570 cm^{-1}. They are represented by

stretching vibrations in this region (Figures 7 and 8) [40-42]. Oxidation process by potassium permanganate leads to the disappearance of this band [39,40]. They depicted evident changes in disulphide structure of wool and their content after oxidation process. These results are in consistent with previous findings [39,40]. The stability of keratin is clearly caused by the presence of disulphide bonds. Some other peaks that indicate the sulfur containing chemical groups usually appear between 900 and 1300 cm^{-1} [40,41].

Main parts of the wool structure consist of cuticle, cortex, and medulla [16] and its functional groups are carboxyl (-COOH), amino (-NH_2), and hydroxyl groups (-OH) [16]. The regions of amide I and amide II vibrations usually are ~1650-1730 cm^{-1} and ~1500-1550 cm^{-1}, respectively (Figure 9) [16,36,43]. Amide I mode is predominantly the peptide carbonyl stretching vibration of the CONH unit together with an out-of-phase CN stretching component and a small contribution from the CCN deformation [43]. NH_3^+ group corresponds to a wide band at 3100-2700 cm^{-1} (asymmetric ν_{NH} and symmetric ν_{NH} vibrations) [43]. The amide II mode is predominantly NH in-plane bending plus CN stretching contribution, but it always has a significant contribution from CC stretching and smaller contributions from the CO in-plane bend and NC stretch [43].

Peaks in the region of ~980-1100 cm^{-1} are related to S-O bond, whose content increased, because of cysteic acid residues that are produced through oxidation process [43]. According to Figure 9 cross-linking agent reacts with -OH and -NH_2 groups of wool. At the region of 1600-1640 cm^{-1}, there are peaks related to C-O, and at around 1533 cm^{-1}, the peaks of C-N stretching and N-H appear. These bonds have been affected through oxidation and also treatment in the impregnating bath. This means that the -COOH group of BTCA and O-H, -NH_2 groups of wool fiber altered to -COO and/or -CONH; in other words, cross-linking reactions occurred between BTCA and wool [16]. The peak was observed at about 3200-3500cm^{-1} (Figure 10). Serine peaks appear usually at around 3400 cm^{-1} [43]. Some peaks of amide side chains can be seen at about 3200 cm^{-1} [43]. The explanation of these peaks in above region is difficult because of the wide band of -OH in the vicinity of 3400 cm^{-1} [43].

SEM Images

The surfaces of the treated fabrics were observed using

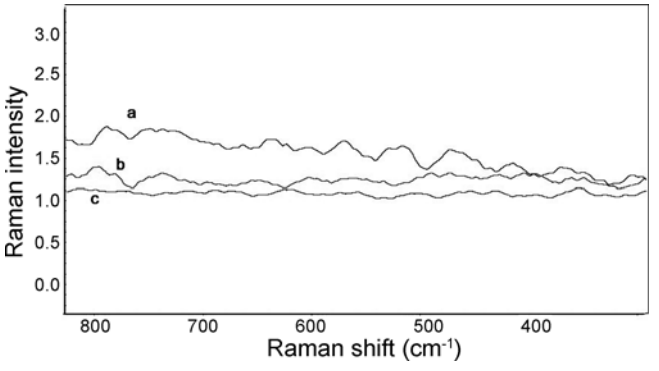

Figure 7. Raman spectra of wool fabric over 400-800 cm^{-1}; (a) raw wool, (b) oxidized wool, and (c) treated wool with TiO_2, BTCA, and SHP.

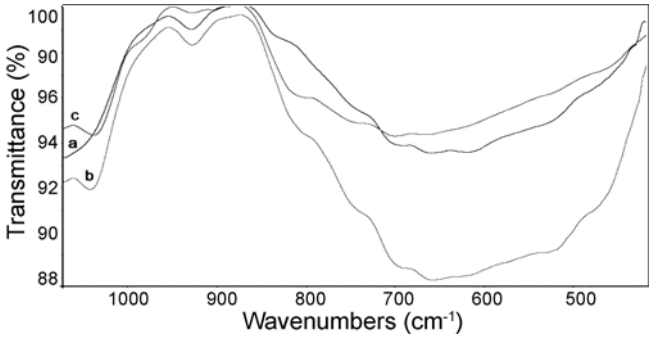

Figure 8. FT-IR spectra of wool fabric over 500-1000 cm^{-1}; (a) raw wool, (b) oxidized wool, and (c) treated wool with TiO_2, BTCA, and SHP.

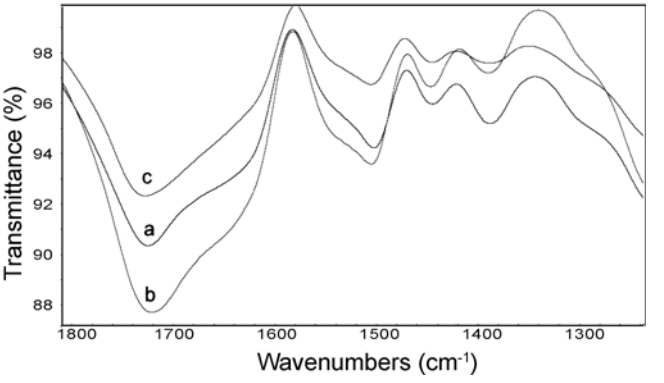

Figure 9. FT-IR spectra of wool fabric over 1300-1800 cm^{-1}; (a) raw wool, (b) oxidized wool, and (c) treated wool with TiO_2, BTCA, and SHP.

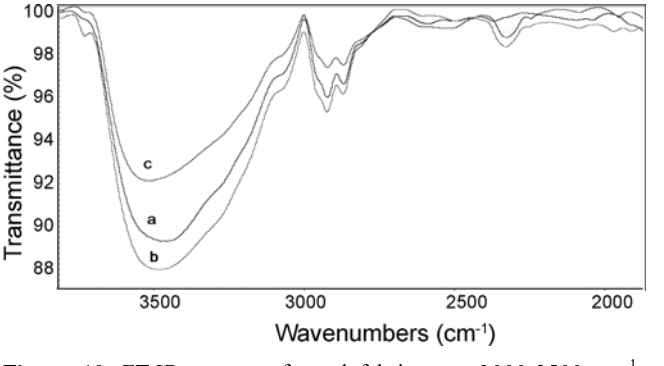

Figure 10. FT-IR spectra of wool fabric over 2000-3500 cm^{-1}; (a) raw wool, (b) oxidized wool, and (c) treated wool with TiO_2, BTCA, and SHP.

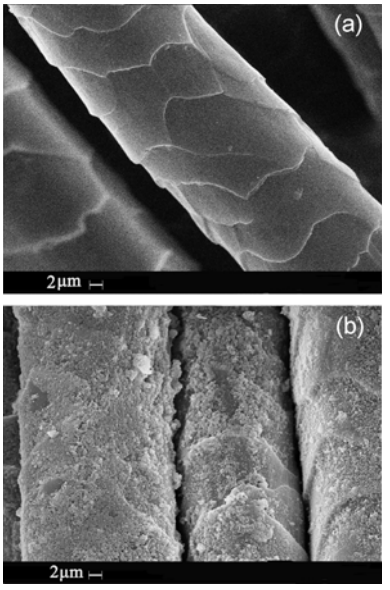

Figure 11. SEM images of treated wool with TiO_2, BTCA, and SHP; (a) raw wool and (b) oxidized wool treated with TiO_2 (×2000).

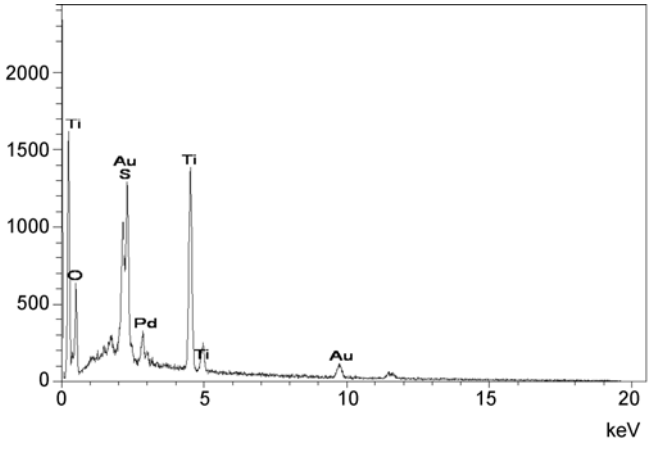

Figure 12. EDS pattern of nano TiO_2 treated sample.

SEM microscopy. In Figures 11(a) and 11(b), SEM micrographs show the scales of raw wool and nano-scaled TiO_2 particles on wool samples, respectively. The aggregated nano-particles on wool surface can be seen in Figure 11(b). The large particles will be easily removed from the fiber surface while the small particles can penetrate into the fabric matrix and adhere stronger on fabric surface. SEM pictures of raw and treated samples in Figure 11 show that the surfaces of the treated samples are covered by titanium dioxide nano particles.

EDS Pattern

EDS (energy-dispersive X-ray spectrometry) pattern (Figure 12) of the treated samples proved the existence of TiO_2 on the fabric surfaces and some other elements such as S, O, and C. EDS is an analytical technique used for the elemental analysis or chemical characterization of a sample. As a type of spectroscopy, it relies on the investigation of a sample through interactions between electromagnetic radiation and matter, analyzing X-rays emitted by the matter in response to being hit with charged particles. Its characterization capabilities are due in large part due to the fundamental principle that each element has a unique atomic structure allowing X-rays which are characteristic of an element atomic structure to be distinguished uniquely from each other. The signal-to-noise ratio for the resulting EDS patterns was highly related to particle size. EDS patterns for smaller particles produced better signal-to-noise ratios that were independent of particle size.

Conclusion

In this study an approach was examined to prevent wool fabric from photo-yellowing. The results revealed that TiO_2 nano particles clearly absorbed UV radiations. These nano particles were applied on wool surface and as a result the rate of photo-yellowing decreased. In order to increase the absorption and durability of titanium dioxide nano particles, BTCA was used as a cross-linking agent accompanied by sodium hypophosphite as a catalyst. RSM was employed to obtain a better evaluation on the effects of each factor on the whiteness and yellowness. The optimum amounts of independent variables for achieving the best response surfaces were determined. The results also indicated that by increasing the amount of nano titanium dioxide in the impregnating bath the absorption of nano TiO_2 on wool surface increased followed by a rise in the UV protection property of the treated samples, in other words, the wool color variation decreased.

References

1. M. L. Kaariainen, T. O. Kaariainen, and D. C. Cameron, *Thin Solid Films,* **517**, 6666 (2009).
2. A. Fujishima and K. Honda, *Nature*, **238**, 38 (1972).
3. A. Fujishima and X. Zhang, *C. R. Chim.*, **8**, 750 (2005).
4. A. L. Castro, M. R. Nunes, M. D. Carvalho, L. P. Ferreira, J. C. Jumas, F. M. Costa, and M. H. Florencio, *J. Solid State Chem.*, **182**, 1838 (2009).
5. I. K. Konstantinou and T. A. Albanis, *Pure Appl. Chem.*, **72**, 1256 (2000).
6. J. M. Herrmann, *Catal. Today*, **53**, 115 (1999).
7. H. U. Zhang, K. R. Millington, and X. Wang, *Polym. Degrad. Stabil.,* **94**, 278 (2009).
8. X. D. Chen, Z. Wang, Z. F. Liao, Y. Mai, and M. Q. Zhang, *Polym. Test.,* **26**, 202 (2007).
9. R. S. Davidson, *J. Photoch. Photobiol. B*, **33**, 3 (1996).
10. K. R. Millington and K. J. Kirschenbaum, *Color. Technol.*,

118, 7 (2002).
11. J. A. Maclaren and B. Milligan, "Wool Science", Science Press, Maririckville, NSW, 1981.
12. H. Zahn, J. Fohles, M. M. Nienhaus, and M. Schwan, *Ind. Eng. Chem. Prod. Res. Dev.*, **19**, 496 (1980).
13. D. J. Raven, C. Earland, and M. Little, *Biochim. Biophys. Acta*, **251**, 96 (1971).
14. C. H. Nicholls, in "Developments in Polymer Photochemistry" (N. S. Allen Ed.), Vol. 1. pp.125-144, Applied Science Publishers, Barking, U.K., 1980.
15. K. R. Millington, *Color. Technol.*, **122**, 301 (2006).
16. K. Schafer, "Investigation to Stabilize Optically Brightened Wool Against Light Damage", Proceedings of 8th International Wool Textile Research Conference, Christchurch, NZ, Vol. IV, pp.250-259, 1990.
17. K. Qi, W. A. Daoud, J. H. Xin, C. L. Mak, W. Tang, and W. P. Cheung, *J. Mater. Chem.,* **16**, 4567 (2006).
18. W. A. Daoud, S. K. Leung, S. K. Tung, J. H. Xin, K. Cheuk, and K. Qi, *Chem. Master.*, **20**, 1242 (2008).
19. M. Montazer and E. Pakdel, *Photochem. Photobiol.*, **86**, 255 (2010).
20. M. Montazer and E. Pakdel, *J. Text. Inst*., accepted for publication.
21. C. C. Wang and C. C. Chen, *J. Appl. Polym. Sci.*, **97**, 2450 (2005).
22. C. Q. Yang, *Text. Res. J.,* **67**, 334 (1997).
23. B. J. Trask-Morrel and A. Kottes, *Text. Res. J.,* **67**, 846 (1997).
24. W. Xu and T. W. Shyr, *Text. Res. J.*, **70**, 8 (2000).
25. W. Xu and Y. Li, *Text. Res. J.*, **70**, 588 (2000).
26. D. M. Lewis and B. Voncina, *J. Appl. Polym. Sci.*, **66**, 171 (1997).
27. B. A. Kotte, *Text. Chem. Color.*, **22**, 63 (1990).
28. B. Voncina, *Fibres Text. East. Eur.*, **1**, 69 (1996).
29. D. C. Montgomery, "Design and Analysis of Experiments", 4th ed., John Wiley & Sons, USA, 1996.
30. A. Ozer, G. Gurbuz, A. Calimli, and B. Korbahti, *Chem. Eng. J.*, **146**, 377 (2009).
31. R. H. Myers and D. C. Montgomery, "Response Surface Methodology, Process and Product Optimization Using Designed Experiments", 2nd ed., John Wiley and Sons, New York, p.235, 2002.
32. M. Amini, H. Younesi, N. Bahramifar, A. A. Z. Lorestani, F. Ghorbani, A, Daneshi, and M, Sharifzadeh, *J. Hazard. Mater.*, **154**, 694 (2008).
33. A. Kantouch, A. Bendak, and M. Sadek, *Text. Res. J.*, **48**, 619 (1978).
34. S. H. Hsieh, Z. K. Huang, Z. Z. Huang, and Z. S. Tseng, *J. Appl. Polym. Sci.*, **94**, 1999 (2004).
35. G. E. P. Box and N. R. Draper, "Empirical Model-building and Response Surfaces", John Wiley & Sons, New York, 1987.
36. D. Bas and I. H. Boyaci, *J. Food. Eng.*, **78**, 836 (2007).
37. J. Zhu, F. Chen, J. Zhang, H. Chen, and M. Anpo, *J. Photoch. Photobiol. A*, **180**, 196 (2006).
38. H. Yang and S. Zhu, *J. Appl. Polym. Sci.*, **92**, 3201 (2004).
39. W. Xu, G. Ke, J. Wu, and X. Wang, *Eur. Polym. J.,* **42**, 2168 (2006).
40. E. Wojciechowska, M. Rom, A. Włochowicz, M. Wysocki, and A. W. Birczynska, *J. Mol. Struct.,* **704**, 315 (2004).
41. A. T. Tu, R. J. H. Clark, and R. R. Hester (Eds.), "Spectroscopy of Biological Systems", Wiley, New York, p.47, 1986.
42. W. Akhtar, H. G. M. Edwards, D. W. Farwell, and M. Nutbrown, *Spectrochim. Acta A*, **53**, 1021 (1997).
43. A. Pielesz, A. Wlochowicz, and W. Binias, *Spectrochim. Acta A*, **56**, 1409 (2000).